

# UC Irvine

## UC Irvine Previously Published Works

### Title

Electrically tunable lens speeds up 3D orbital tracking

### Permalink

<https://escholarship.org/uc/item/9n25g0s2>

### Journal

Biomedical Optics Express, 6(6)

### ISSN

2156-7085

### Authors

Annibale, Paolo

Dvornikov, Alexander

Gratton, Enrico

### Publication Date

2015-06-01

### DOI

10.1364/boe.6.002181

### Copyright Information

This work is made available under the terms of a Creative Commons Attribution License, available at <https://creativecommons.org/licenses/by/4.0/>

Peer reviewed

# Electrically tunable lens speeds up 3D orbital tracking

Paolo Annibale,<sup>1,2</sup> Alexander Dvornikov,<sup>1,2</sup> and Enrico Gratton<sup>1,\*</sup>

<sup>1</sup>Laboratory for Fluorescence Dynamics, Department of Biomedical Engineering, University of California, Irvine USA

<sup>2</sup>Authors contributed equally to this work  
\*egratton22@gmail.com

**Abstract:** 3D orbital particle tracking is a versatile and effective microscopy technique that allows following fast moving fluorescent objects within living cells and reconstructing complex 3D shapes using laser scanning microscopes. We demonstrated notable improvements in the range, speed and accuracy of 3D orbital particle tracking by replacing commonly used piezoelectric stages with Electrically Tunable Lens (ETL) that eliminates mechanical movement of objective lenses. This allowed tracking and reconstructing shape of structures extending 500 microns in the axial direction. Using the ETL, we tracked at high speed fluorescently labeled genomic loci within the nucleus of living cells with unprecedented temporal resolution of 8ms using a 1.42NA oil-immersion objective. The presented technology is cost effective and allows easy upgrade of scanning microscopes for fast 3D orbital tracking.

©2015 Optical Society of America

OCIS codes: (110.0110) Imaging systems; (180.0180) Microscopy.

## References and links

1. Dupont and D. C. Lamb, "Nanoscale three-dimensional single particle tracking," *Nanoscale* **3**(11), 4532–4541 (2011).
2. N. Chenouard, I. Smal, F. de Chaumont, M. Maška, I. F. Sbalzarini, Y. Gong, J. Cardinale, C. Carthel, S. Coraluppi, M. Winter, A. R. Cohen, W. J. Godinez, K. Rohr, Y. Kalaidzidis, L. Liang, J. Duncan, H. Shen, Y. Xu, K. E. Magnusson, J. Jaldén, H. M. Blau, P. Paul-Gilloteaux, P. Roudot, C. Kervrann, F. Waharte, J. Y. Tinevez, S. L. Shorte, J. Willemsse, K. Celler, G. P. van Wezel, H. W. Dan, Y. S. Tsai, C. Ortiz de Solórzano, J. C. Olivo-Marín, and E. Meijering, "Objective comparison of particle tracking methods," *Nat. Methods* **11**(3), 281–289 (2014).
3. T. Ragan, H. Huang, P. So, and E. Gratton, "3D particle tracking on a two-photon microscope," *J. Fluoresc.* **16**(3), 325–336 (2006).
4. J. Enderlein, "Tracking of fluorescent molecules diffusing within membranes," *Appl. Phys. B* **71**(5), 773–777 (2000).
5. K. Kis-Petikova and E. Gratton, "Distance measurement by circular scanning of the excitation beam in the two-photon microscope," *Microsc. Res. Tech.* **63**(1), 34–49 (2004).
6. F. Cardarelli, L. Lanzano, and E. Gratton, "Capturing directed molecular motion in the nuclear pore complex of live cells," *Proc. Natl. Acad. Sci. U.S.A.* **109**(25), 9863–9868 (2012).
7. V. Levi, Q. Ruan, and E. Gratton, "3-D particle tracking in a two-photon microscope: application to the study of molecular dynamics in cells," *Biophys. J.* **88**(4), 2919–2928 (2005).
8. A. Anzalone, P. Annibale, and E. Gratton, "3D orbital tracking in a modified two-photon microscope: an application to the tracking of intracellular vesicles," *J. Vis. Exp.* **92**, e51794 (2014).
9. C. L. Chiu, M. A. Digman, and E. Gratton, "Measuring actin flow in 3D cell protrusions," *Biophys. J.* **105**(8), 1746–1755 (2013).
10. V. Levi, Q. Ruan, M. Plutz, A. S. Belmont, and E. Gratton, "Chromatin dynamics in interphase cells revealed by tracking in a two-photon excitation microscope," *Biophys. J.* **89**(6), 4275–4285 (2005).
11. P. Annibale and E. Gratton, "Advanced fluorescence microscopy methods for the real-time study of transcription and chromatin dynamics," *Transcription* **5**, e28425 (2014).
12. L. Lanzano, M. A. Digman, P. Fwu, H. Giral, M. Levi, and E. Gratton, "Nanometer-scale imaging by the modulation tracking method," *J Biophotonics* **4**(6), 415–424 (2011).
13. B. F. Grewe, F. F. Voigt, M. van 't Hoff, and F. Helmchen, "Fast two-layer two-photon imaging of neuronal cell populations using an electrically tunable lens," *Biomed. Opt. Express* **2**(7), 2035–2046 (2011).
14. H.-C. Lin, M.-S. Chen, and Y.-H. Lin, "A Review of Electrically Tunable Focusing Liquid Crystal Lenses," *Transactions on Electrical and Electronic Materials* **12**(6), 234–240 (2011).

15. H. Oku, K. Hashimoto, and M. Ishikawa, "Variable-focus lens with 1-kHz bandwidth," *Opt. Express* **12**(10), 2138–2149 (2004).
  16. J. M. Jabbour, B. H. Malik, C. Olsovsky, R. Cuenca, S. Cheng, J. A. Jo, Y. S. Cheng, J. M. Wright, and K. C. Maitland, "Optical axial scanning in confocal microscopy using an electrically tunable lens," *Biomed. Opt. Express* **5**(2), 645–652 (2014).
  17. A. Maizel, D. von Wangenheim, F. Federici, J. Haseloff, and E. H. Stelzer, "High-resolution live imaging of plant growth in near physiological bright conditions using light sheet fluorescence microscopy," *Plant J.* **68**(2), 377–385 (2011).
  18. J. B. Sibarita, "Deconvolution microscopy," *Adv. Biochem. Eng. Biotechnol.* **95**, 201–243 (2005).
  19. V. Dion and S. M. Gasser, "Chromatin movement in the maintenance of genome stability," *Cell* **152**(6), 1355–1364 (2013).
  20. C. C. Robinett, A. Straight, G. Li, C. Willhelm, G. Sudlow, A. Murray, and A. S. Belmont, "In vivo localization of DNA sequences and visualization of large-scale chromatin organization using lac operator/repressor recognition," *J. Cell Biol.* **135**(6), 1685–1700 (1996).
  21. F. R. Neumann, V. Dion, L. R. Gehlen, M. Tsai-Pflugfelder, R. Schmid, A. Taddei, and S. M. Gasser, "Targeted INO80 enhances subnuclear chromatin movement and ectopic homologous recombination," *Genes Dev.* **26**(4), 369–383 (2012).
  22. H. Hajjoul, J. Mathon, H. Ranchon, I. Goiffon, J. Mozziconacci, B. Albert, P. Carrivain, J. M. Victor, O. Gadal, K. Bystricky, and A. Bancaud, "High-throughput chromatin motion tracking in living yeast reveals the flexibility of the fiber throughout the genome," *Genome Res.* **23**(11), 1829–1838 (2013).
- 

## 1. Introduction

Tracking individual fluorescent particles within a biological sample is a topic of active research in Biophotonics [1]. Many methodologies have been developed over the last two decades to track fluorescent particles in three dimensions using a microscope.

Most of these methods utilize wide field imaging systems, employing cameras to perform fast tracking in 2D and reconstructing particles trajectories by connecting the dots [2]. Modifications in the microscope detection optics are generally adopted in order to perform tracking in the axial direction. Laser scanning microscopes (either confocal or 2-photon) can follow a particle in 3D by performing a time sequence of z-stacks. This process has a low frequency response and a time resolution of the order of 10 Hz or less and can be used if the tracked particle is kept at the center of a small raster imaging region by an active feedback mechanism [3].

3D orbital particle tracking is a lock-in method allowing a frequency response in excess of 100 Hz [4]. By using a laser scanning system, a circular orbit is performed around the fluorescent particle instead of a raster scan. The fluorescence intensity modulation along the orbit is used to precisely localize the particle position [5]. The localized position of the particle then can be used to actuate the microscope scanners and re-center the orbit on the particle position. The period of the  $xy$  circular orbit of the focused laser beam is limited by the frequency response of the galvanometer mirrors, and frequencies of the order of 1kHz or higher can be achieved [6].

A current limitation of the method is the limited frequency response for tracking along the axial dimension ( $z$ ) as compared to the  $x$ - $y$  plane. While tracking in the image plane relies on fast galvo scanners to steer the beam, axial tracking is usually performed by moving the objective lens with a piezo stage, which results in a slower frequency response [7]. Also, fast movement of objective lens prevents the use high NA (Numerical Aperture) oil immersion objectives.

To localize the particle along the axial direction, the commonly used approach is to perform subsequent orbits above and below the tracked object, the normalized difference of the measured intensity (axial modulation) is an indication of the  $z$ -position of the particle. It is clear that a 3D localization is at least two times slower than a 2D localization due to the difference in response of the  $z$ -piezo actuator and also because of the  $z$ -extent of the PSF. The step response time of a typical commercial piezo-stage is of the order of a 10-20 ms, although top-end models may attain a rise time as low as a few ms. A slower rise time leads to lower axial modulation and decreases the precision of axial tracking.

Furthermore, the practical extent of the axial tracking is limited by the ability of a mechanical scanner, such as a piezo-scanner, to displace a microscope objective (typical

range is 100  $\mu\text{m}$ ), as well as by the working distance of the objective. Due to the relatively fast movement needed in the z direction only air or water objectives can be used.

3D orbital particle tracking has been successfully applied to study a number of biological systems and processes, including the progression of molecular motors along the cytoskeleton [8], the actin flow within cell protrusions [9], the tracking of fluorescently labeled genetic loci [10,11] and others. In each of these applications, the speed of the particle motion can be on the order of  $\mu\text{m/s}$ . In addition, the 3D orbital tracking method combined with a higher frequency modulation of the orbit radius, namely the nano-Scale Precise Imaging by Rapid Oscillation (nSPIRO) method can be employed for the morphological reconstruction of arbitrary fluorescent shapes within the orbit [12]. The plane of the orbit can be arbitrarily changed to follow the geometry of the structure being tracked.

Therefore, any method that can improve the frequency response of orbital tracking and increase the rapidity of orbital switching represents an important advancement. Various technologies were utilized for fast focus tuning without mechanical movement, such as electrowetting, liquid crystals, MEMS, piezoelectric and electro-mechanical devices, as already addressed by [13]. The response time for such devices may vary from reasonably slow, a few hundred ms for liquid crystal lenses [14] to 1ms for piezo-hydraulic actuation [15].

In this paper we present a method that allows us to change the position of the focused laser beam along the axial direction at increased speed and over an extended range with respect to the piezo actuator. For this purpose we employed a commercially available electrically tunable lens (ETL) that allows fast switching of the imaging plane without mechanical displacement of the objective.

This lens was successfully used in the past to achieve fast multiplane imaging of neuronal cell populations in a multi-photon microscope [13] and in axial confocal microscopy [16]. We demonstrate the advantages of this approach for orbital tracking by comparing experimental results obtained with the ETL and a piezo actuator. We demonstrate the application of the improved setup to (i) the shape reconstruction of the root and root hair of an Arabidopsis Thaliana plant growing in an agar matrix, based on its autofluorescence, (ii) the high speed tracking of two fluorescently labeled genetic loci moving within the nucleus of a living cell.

## 2. Materials and methods

### 2.1 Experimental setup

Most experiments were performed using a custom built two-photon microscope based on the frame of a Zeiss 135 Axiovert that employs two galvo laser beam steering mirrors (Cambridge Technology) for xy scanning. The steering of the focal point in the axial (z) direction was performed by attaching an objective lens to the piezo-stage positioner NanoF-100 (MadCity Labs) or to ETL (Optotune EL-10-30) assembly (see below) that changes the laser beam divergence at the back aperture of the objective. Both the piezo-stage and ETL were controlled by an ISS 3-axis card (ISS, Urbana-Champaign, IL).

To generate a divergent or convergent laser beam at the rear aperture of the microscope objective we utilized a combination of the ETL, tunable in the range of + 50 to + 200 mm focal length, with a -75 mm focal length plano-concave offset lens (Newport, KPC019AR.14), as described in [13]. The ETL and offset lenses were placed in direct contact in the custom made holder, which is constructed to minimize overall thickness of the assembly (Fig. 1). The holder has RMS threads and can be directly attached between the microscope turret and objective instead of the piezo-stage. Technical characteristics of ETL can be found on the manufacturer website ([www.optotune.com](http://www.optotune.com)) in the provided datasheet.

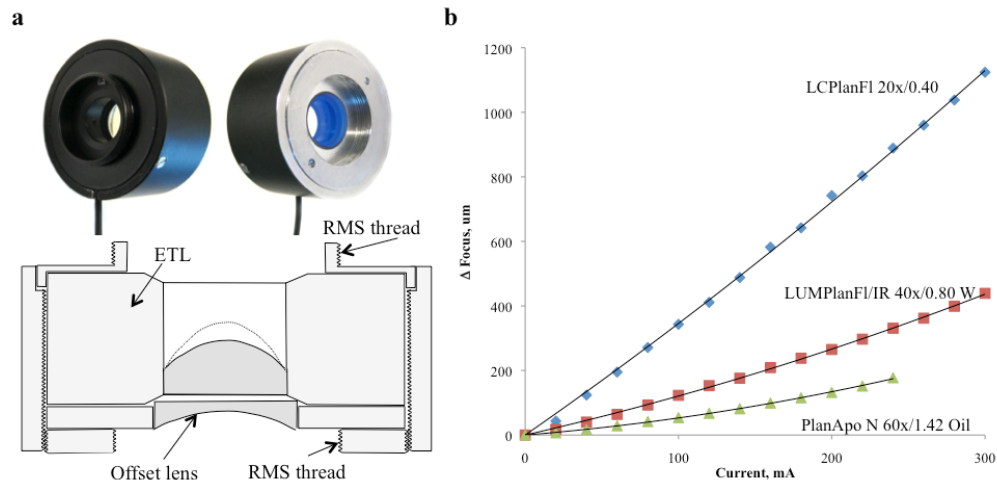


Fig. 1. a) Picture and schematics of the casing of the electrical lens, that allows it to be installed at the rear of any RMS objective. b) The focal length changes with the Current, with a slope depending on the magnifying power of the objective. A 20x objective yields an axial field of view of over one mm, which reduces to 200  $\mu\text{m}$  if a 60x objective is used.

Tracking experiments were performed using Olympus LCPlanFI 20x/0.40; LUMPlanFI/IR 40x/0.80 W and PlanApo N 60x/1.42 Oil Objectives. Figure 1(b) shows the dependence of focal point displacement vs. current applied to ETL for various microscope objectives used in experiments. Excitation light was generated by a Ti-Sa Femtosecond pulsed laser (Mai Tai, Spectra Physics).

## 2.2 Materials

*Arabidopsis Thaliana* seeds were sterilized using 15% bleach solution and washed 10 times in sterile distilled water and placed at 4° C for 48 h. The seeds were then placed on standard Murashige and Skoog (MS) plant growth media with 1% agar cast in a 35 mm Glass bottom dish from MatTek Corporation and grown for 4 days in a constant light condition.

U2OS cells containing 256 Lac operator cassette (a kind gift of Dr. Kyoko Yokomori and Dr. Xiangduo Kong) stably integrated within the genome were cultured using DMEM (LifeTechnologies) supplemented with 10% FBS and 1% Penicillin/Streptomycin. Cells were transfected with Lipofectamine 2000 (LifeTechnologies), according to the manufacturer instructions, using 2  $\mu\text{g}$  of LacI-GFP DNA.

## 3. Results

### 3.1 Comparing the performance of the electrical lens and a piezo-stage

To compare response times of the ETL and the piezo-stage, a fast photodiode (Thorlabs DET10A) was used to detect light modulation induced by the change in the axial position of the laser beam focal point due to ETL voltage modulation. The piezo-stage driver provides an actual position of the piezo-stage. The relationship between scanning period and modulation of the axial oscillation using a piezo stage is clearly illustrated in Fig. 2(a). It shall be noted that the piezo step response time is independent of the actual amplitude of its z-motion for the typical  $\mu\text{m}$ -sized scales required to switch between the orbits.

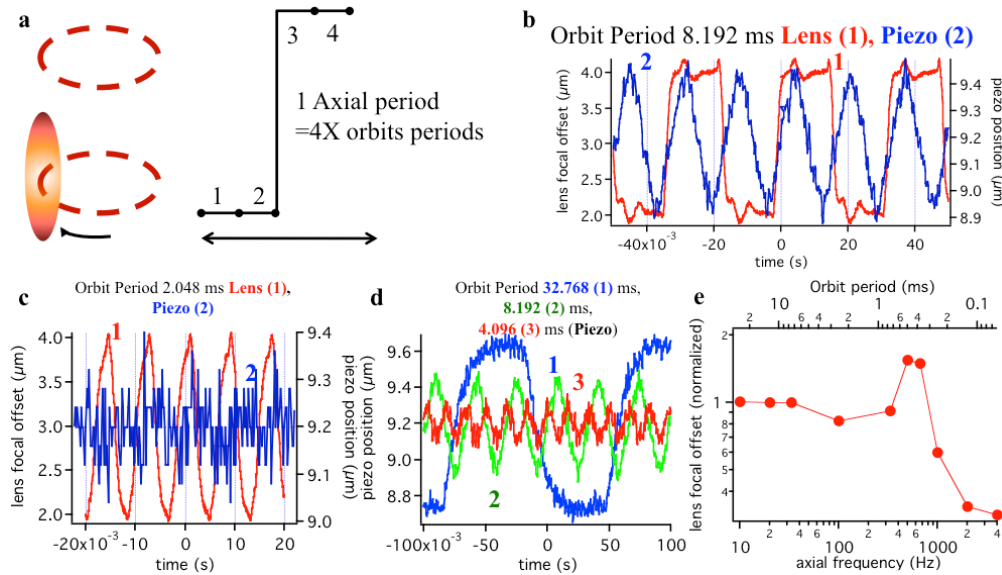


Fig. 2. Comparative performances of an objective piezo-stage and of the electrical lens. a) Schematics of the orbital tracking configuration. A full 3D tracking period is achieved by performing 4 radial periods: 2 above and 2 below the particle. b) Piezo and lens performance compared for an orbit period of 8.192 ms. The up-down period for orbital tracking 32.77 ms. Comparing the displacement of the focal plane achieved by movement of the objective (Piezo, blue line, 2) and by the use of the ETL (Lens, red line, 1) c) Comparing piezo and lens performance for an orbital period of 2.048 ms. d) Demodulation of the piezo response for decreasing orbit period. The ideal square wave response turns to a triangular wave response, as the device is not able to perform the entire axial excursion in the required time e) Lens focal offset of ETL response for increasing axial frequency (i.e. decreasing orbit period, as indicated in the top axis). A resonance at about 500Hz is observed.

Figure 2(b) compares responses of the ETL and the piezo-stage for an orbital scanning radial period of 8.192 ms. The focal point displacement achieved by the ETL (red line) has a frequency response comparable to the square wave input scanning signal, while the step response time of the piezo stage is slower and it cannot follow the fast changes of the square wave input scanning signal (blue line). This reduces the effective axial modulation, which is calculated from the difference in intensity between the upper and lower orbits.

At shorter periods (2.048 ms) a drastic demodulation of the piezo response can be observed (Fig. 2(c)). The ETL response deviates from the square wave but is not demodulated and still allows clearly identifying an upper and lower period.

The demodulation of the piezo displacement for increasingly shorter periods (Fig. 2(d)) is one of the most significant limitations for ms-resolution 3D particle tracking. As illustrated in Fig. 2(e) this is not significantly affecting the ETL response for orbit period as low as 0.7 ms.

To compare further 3D orbital tracking performance of the ETL and the Piezo-stage, we performed tracking of a 1  $\mu\text{m}$  fluorescent bead (Tetraspeck, LifeTechnologies) that was moved in a predetermined spiral pattern by means of a motorized positioning stage (Applied Scientific Instruments, MS2000). 3D orbital tracking of the moving bead was performed using an orbital period of 2.048 ms. The spiral had a radius of 7  $\mu\text{m}$  in the xy plane and extended to about 30  $\mu\text{m}$  in the axial direction. The instantaneous bead velocity is approximately 5  $\mu\text{m/s}$ .

Figure 3 illustrates the reconstructed 3D trajectories of the tracked bead by means of either the piezo-stage (Fig. 3(a)) or the ETL (Fig. 3(b)) respectively. To benchmark the two methods we plotted the distribution of the deviation of the measured positions of the bead from the x,y,z position of the scanner (Fig. 3(c)).

The smaller tails of the frequency distribution illustrate that the ETL has a superior performance with respect to the piezo-stage for 3D fast-tracking applications. As a drawback,

we observed a deformation of the field of view as a function of the z-position when using the ETL. This is probably due to a slight mechanical misalignment that may occur between the electrical lens and its casing.

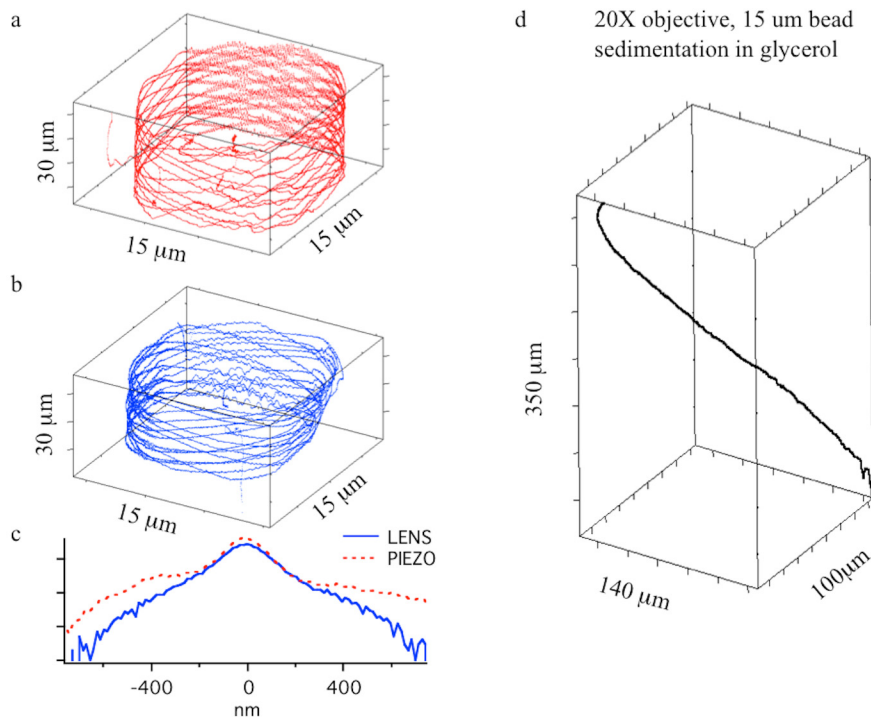


Fig. 3. a) Reconstructed trajectory of a 1 μm fluorescent bead moved in a periodic 3D spiral pattern by the stepper-motor stage over a FOV of 15 μm (x-y) and 30 μm (z). Axial tracking is performed using the objective piezo-stage. b) Reconstructed trajectory of a 1 μm fluorescent bead moved in a periodic 3D spiral pattern by the stepper-motor stage over a FOV of 15 μm (x-y) and 30 μm (z). Axial tracking is performed using the ETL. For both experiments reported in a and b a 40x 0.8 NA water objective was used. c) Frequency distribution (log-scale) of the measured distance between scanner position and localized particle position for the test trajectories generated in a and b. d) Sedimentation profile of a 15 μm fluorescent bead over an axial range of 350 μm followed using the electrical lens and a 20x 0.4NA objective.

Another significant advantage of using the ETL for orbital tracking is its ability to move the focal plane over a much wider range than allowed by the movement of the objective with a piezo-stage, which is typically limited to 100–200 μm for most piezo-stage actuators.

To estimate the ability of ETL to track particles over a large axial distance we conducted 3D orbital tracking of a 15 μm fluorescent bead in 80% water-glycerol mixture. Figure 3(d) illustrates that the bead sedimentation process can be tracked for more than 350 μm in the axial direction when the ETL is used in combination with a 20x 0.4NA air objective. If compared to other 3D fluorescent particle tracking approaches this is an unprecedented range.

### 3.2. Tracking large structures in 3D

To test the advantage offered by the ETL in providing an extended axial field of view, we performed 3D tracking reconstruction (nSPIRO) of large biological structures. The nSPIRO method is a variant of the orbital tracking method that reconstructs the shape of a fluorescent object besides tracking its movement.

The foundations of the technique have been previously described in detail [12]. Briefly, the orbiting beam is oscillated with a higher frequency along the radial direction. The modulation of the fluorescence signal along the radial direction provides the additional

information needed to reconstruct not only the center, but also the shape of the distribution of fluorophores within the orbit.

In addition, since the orbital tracking method is fully compatible with 2-photon excitation, it allows exciting fluorescence in thick or scattering samples. We were able to reconstruct the shape of large *Arabidopsis Thaliana* roots (Fig. 4(a)) in agar gels by orbital tracking using the ETL in our custom-built 2-photon laser-scanning microscope setup. *Arabidopsis* roots grow up to a few millimeters in the Agar gel, developing characteristic hairs around the main root (Fig. 4(b)).

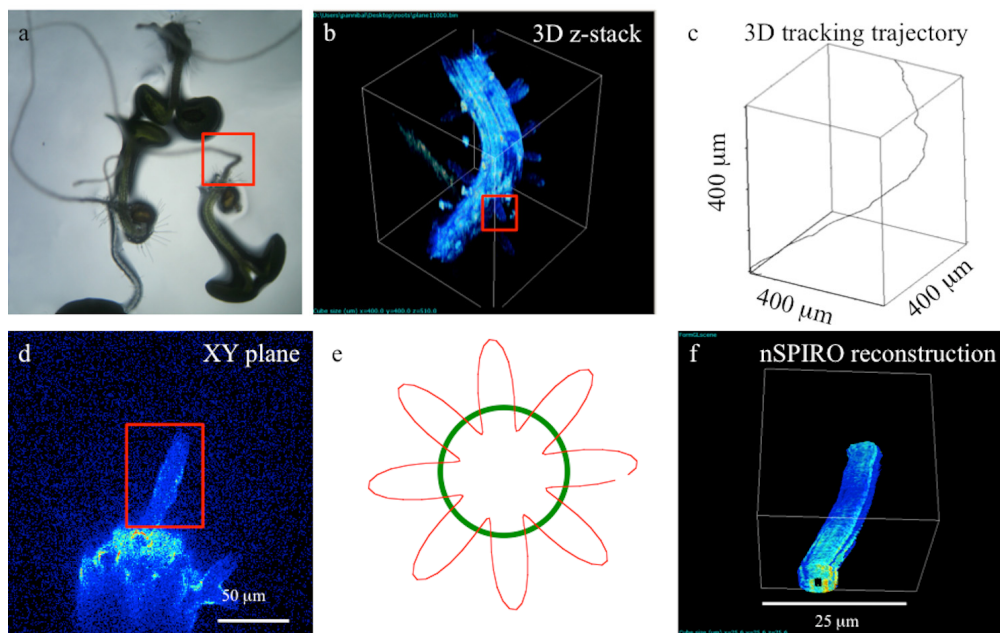


Fig. 4. Bottom-up Picture of *Arabidopsis Thaliana* plants rooting in an agar plate with a glass-bottom. b) 3D reconstruction of a portion of the root from a 2-photon excitation z-stack performed by using 750 nm excitation. c) Trajectory of the root axis reconstructed from 3D orbital particle tracking, performed by ramping the position of the collimated laser beam along the axial direction using the ETL over a range exceeding 400  $\mu\text{m}$ . d) Z-Section of a root highlighting a root hair protrusion. e) Pattern of the rosette orbit performed in the XZ plane to reconstruct the shape of the root hair. f) nSpiro reconstruction of the root hair. All experiments were performed with a 20x 0.4NA objective.

3D images of the root formation have been obtained previously using SPIM technology [17]. The 3D tracking technique is able to follow the shape of individual roots and reconstruct the 3D structure of individual root hairs within a few seconds without any particular sample preparation requirement or special sample holder.

In order to obtain the reconstructed profile of the root illustrated in Fig. 4(c) the focused laser beam is orbited in the xy plane while its position along z follows a linear ramp. The ETL allows following the shape of *Arabidopsis* root over a 400  $\mu\text{m}$  field of view based on the autofluorescence elicited by 2-photon excitation at 750 nm wavelength.

For 3D shape reconstruction we first identified the root hair by conventional 3D raster scan imaging. Then the nSPIRO method is applied: briefly, the laser beam is orbited in a plane (x-z in this case), while the position of the focused beam is ramped along the third dimension (y). The orbit shape is radially modulated to resolve the distance between the beam and the surface and to detect potential changes in the shape. A feedback on the modulation allows adjusting the orbit radius to follow changes in the shape and thickness of the object being tracked. We modulate the orbital radius using the 8-th harmonic of its period, which

results in a *rosette* shape of the orbit (Fig. 4(e)). The following parameters were used: 16.4 ms per orbit period; 128  $\mu\text{s}$  per point (128 points/orbit).

The results of 3D reconstruction of a root hair shape are shown in Fig. 4(f), illustrating how both the shape of the root hair as well as the fluorescence distribution along the root surface can be reproduced. nSPIRO reconstruction of an individual root-hair was possible over a field of view of 25  $\mu\text{m}$ .

In this application, the advantage of using the ETL instead of the piezo-stage is that the ETL allows a faster movement of the microscope focused laser beam in the x-z plane, which is required to maintain the symmetry of the *rosette* orbit illustrated in Fig. 4(e).

### 3.3. Tracking the diffusion of genetic loci at sub-10ms temporal resolution

3D orbital particle tracking using oil immersion objectives with a piezo-stage is not possible, since the mechanical movement of objective in the viscous oil media introduces vibrations that will affect the point spread function [18]. Using high magnification and high NA objectives however is advantageous for single cell level studies, where the increment of the NA results in increased photon collection and a narrower PSF.

The use of the ETL allowed us performing fast 3D particle tracking using a high numerical aperture oil immersion objective (Olympus PlanApo N 60x/1.42 Oil) to track fluorescently labeled genetic loci.

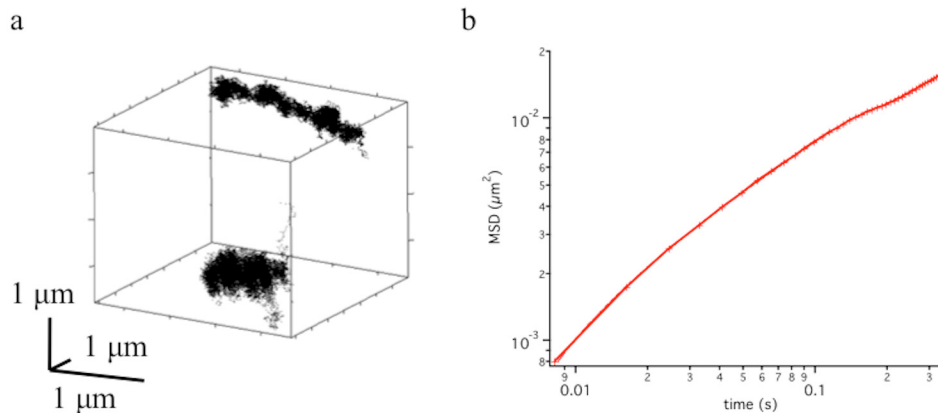


Fig. 5. a) Trajectory of two fluorescently labeled DNA loci tracked in 3D using a 60x 1.42 NA oil immersion objective in combination with the ETL. b) Mean Squared Displacement (MSD) of the distance difference between the two loci.

The importance of measuring the 3D motion of individual chromatin regions could not be overstated. The way a portion of the chromatin fiber can move with respect to its surroundings can reflect its regulatory function, whether a DNA sequence is transcriptionally active or whether DNA damage has occurred, to name only a few important cases [19]. Many studies of chromatin 3D mobility have been performed over the years using cell lines where repeats of Lac operator cassette have been stably inserted within the genome [20]. The site can be fluorescently labeled by transiently transfecting a LacI-GFP chimera.

Similar systems have been investigated in the past by means of fluorescent particle tracking techniques, such as spinning disk 3D time-lapse imaging. The best tracking speed achieved in 3D has been, however, of the order of one localization per second [21], and localization rates in the 10-100 ms range have been so far only achieved in 2D [22].

We set to follow two fluorescently labeled loci within the same cell in 3D at a rate of 125 Hz (Fig. 5(a)). The use of a high NA oil objective allowed us maximizing the number of collected photon from the each of the fluorescently labeled loci (each containing 256 Lac operator repeats), while tracking with a temporal resolution of 4 ms in the x-y plane and 8.1 ms fully in 3D.

Looking at their relative motion, which is unaffected by overall displacements of the nucleus, cell or even a drift of the microscope, we observed the behavior of the Mean Squared Displacement vs. time curve below 50 nm displacements and 10 ms timescales.

#### 4. Summary

By combining the ETL as a fast axial scanning device with galvanometer scanner mirrors we have reported an effective, and low cost method to improve on the current temporal resolution of 3D orbital particle tracking experiments.

The most significant advantages achieved using the ETL are the extended axial range (few hundred micrometers) and the much improved step response time (2.5 ms) with respect to standard piezo stages (~15 ms for the nanoF-100 used in our setup). Although the rise time of the lens is 2.5 ms and the settle time is 15 ms, for the purpose of orbital tracking we could still maintain an acceptable modulation down to oscillation periods of the order of 1-2 ms.

The ETL lens allowed us tracking in 3D over a range of over 300  $\mu\text{m}$  when used in combination with a 20x 0.4 NA air objective.

The ETL displayed also an excellent performance for tracking fluorescent particles moving at high speed (up to 5  $\mu\text{m/s}$ ) in 3D when using a high magnification 40x 0.8 NA water objective and a 60x 1.42 NA Oil objective.

The advantage of using the ETL in two specific applications was then demonstrated. First we demonstrated that the extended axial range can be exploited to follow the organization of large objects, such as the root system of *Arabidopsis Thaliana* embedded in Agar gel. Furthermore, the increased frequency response in the axial direction allowed using the nano-imaging feature of 3D orbital tracking, the nSPIRO method, to reconstruct the shape of a root hair extending perpendicular to the optical axis of the system.

Second, we showed that the ETL can be used in conjunction with a high NA, oil based objective, to follow the MSD of individual genetic loci diffusing within the nucleus of a living cell at a temporal resolution that was so far achieved only to observe the 2D projection of this motion.

As it was mentioned above, the use of high NA oil objectives is only possible when ETL is used for tracking, because it does not involve mechanical movement of the objective, while the use of oil objectives with a piezo stage is restricted by its movement in a viscous medium.

We should mention here that the possibility of switching the focal plane by means of a variable focal length device at the back focal plane of the objective involves certain tradeoffs. Some of them were extensively addressed by Grewe et al. [13], in particular the change of field of view and effective NA with focal plane displacement, as well as the focal drift that may occur due to various temperature effects on the ETL focal length, if temperature is not precisely controlled. However, we should also mention that for our application in the 3D orbital tracking, the fast modulation of the axial position of the orbit is not affected by these artifacts. These problems with the ETL appear for large axial displacement of the imaging plane that in our application could be compensated by an active correction of the  $x,y,z$  position of the sample stage, in order to maintain the tracked particle approximately in the center of the lateral and axial field of view. Similar considerations also apply for most optical aberrations, including Coma, which becomes significant only for large off-axis distances. Circularly symmetric aberrations such as spherical aberration do not affect the symmetry of the tracking process.

Orbital tracking has been demonstrated in multiple biological settings. In particular, it was used since 2005 to follow fluorescently labeled genes using the Lac Operator-Repressor system [10], endosomal vesicles [8], nuclear pore complexes [6] and even kidney cells microvilli [12].

The introduction of the electrical lens extends the applicability of 3D orbital tracking in two distinct directions. The first one is to follow particles moving across large axial distances within biological samples, such as plants or tissues where displacements of a few hundred micrometers could easily occur. In this respect, the fact that the ETL allows to change focal plane without movement of the objective will be of great advantage in instances where the

objective is in direct contact with the sample, such is the case for tissue or live animals, where a mechanical movement may deform the sample. The second direction is to improve the overall temporal resolution and stability of particle tracking. This latter improvement is going to affect all 3D particle tracking applications, from vesicular transport to nuclear dynamics, with a particular emphasis on the ability to track particle diffusion in 3D at a temporal resolution below 4 ms.

As usual, the number of photons absorbed by the sample dictates the photobleaching time. In this respect the use of the electrically tunable lens does not alter the considerations already published in previous 3D orbital particle tracking studies.

In summary, the ETL has the potential to be successfully employed to modify existing laser scanning confocal or 2-photon microscopes for fast 3D orbital tracking. The low cost of the lens compared to other devices such as piezo stages makes its application particularly attractive.

### **Acknowledgments**

This work was supported by Grants NIH P41GM103540, P50 GM076516. The authors would like to thank Dr. Christian Poulsen for kindly providing the Arabidopsis Thaliana samples and Dr. Xiangduo Kong and Dr. Kyoko Yokomori for kindly providing the U2OS cell line containing the 256 LacO repeats.